

# Rapamycin and Dietary Restriction Induce Metabolically Distinctive Changes in Mouse Liver

Zhen Yu,<sup>1</sup> Rong Wang,<sup>1</sup> Wilson C. Fok,<sup>2</sup> Alexander Coles,<sup>3</sup> Adam B. Salmon,<sup>4,5,6</sup> and Viviana I. Pérez<sup>1,7</sup>

<sup>1</sup>Linus Pauling Institute, Oregon State University, Corvallis.

<sup>2</sup>Department of Geriatric Medicine, Oklahoma University Health Science Center and Oklahoma City VA Medical Center.

<sup>3</sup>Department of Chemistry and Biochemistry, University of Michigan-Flint.

<sup>4</sup>Department of Molecular Medicine,

<sup>5</sup>Barshop Institute for Longevity and Aging Studies, and

<sup>6</sup>Audie Murphy VA Hospital, South Texas Veterans Health Care System, San Antonio, Texas.

<sup>7</sup>Department of Biochemistry and Biophysics, Oregon State University, Corvallis.

Address correspondence to Viviana I. Pérez, PhD, Department of Biochemistry and Biophysics, Linus Pauling Institute, Oregon State University, 307 Linus Pauling Science Center, Corvallis, OR 97331. Email: [viviana.perez@oregonstate.edu](mailto:viviana.perez@oregonstate.edu)

Dietary restriction (DR) is the gold standard intervention used to delay aging, and much recent research has focused on the identification of possible DR mimetics. Energy sensing pathways, including insulin/IGF1 signaling, sirtuins, and mammalian Target of Rapamycin (mTOR), have been proposed as pathways involved in the antiaging actions of DR, and compounds that affect these pathways have been suggested to act as DR mimetics, including metformin (insulin/IGF1 signaling), resveratrol (sirtuins), and rapamycin (mTOR). Rapamycin is a promising DR mimetic because it significantly increases both health span and life span in mice. Unfortunately, rapamycin also leads to some negative effects, foremost among which is the induction of insulin resistance, potentially limiting its translation into humans. To begin clarifying the mechanism(s) involved in insulin resistance induced by rapamycin, we compared several aspects of liver metabolism in mice treated with DR or rapamycin for 6 months. Our data suggest that although both DR and rapamycin inhibit lipogenesis, activate lipolysis, and increased serum levels of nonesterified fatty acids, only DR further activates  $\beta$ -oxidation of the fatty acids leading to the production of ketone bodies.

**Key Words:** Rapamycin—Dietary restriction—Metabolites— $\beta$ -oxidation.

Received November 13, 2013; Accepted March 18, 2014

Decision Editor: Rafael de Cabo, PhD

THE mammalian Target of Rapamycin (mTOR) is a key pathway that sits at the nexus of eukaryotic cellular responses to nutrients, growth factors, and energy status (1). mTOR forms two different complexes within the cell, mTORC1 and mTORC2, and rapamycin classically has been considered a specific inhibitor of mTORC1. However, chronic treatment with rapamycin also inhibits mTORC2, and studies show that the insulin resistance observed upon chronic treatment with rapamycin is associated with mTORC2 inhibition (2).

Several studies have shown that rapamycin (Rapa) extends life span in several species, including mice (3,4). Rapa appears to be a very promising intervention because it has significant effects on life span even when applied late in life. Furthermore, several reports indicate that chronic treatment with Rapa positively affects many physiological parameters that decline with age (4,5) although there is still some controversy as to whether Rapa increases life span by delaying aging (6). However, in mice and humans, Rapa has potentially negative secondary effects, including glucose intolerance and insulin resistance, making the long-term use of Rapa in humans questionable.

In an effort to dissect whether dietary restriction (DR) and Rapa work through common mechanisms in mice, we have analyzed the transcriptome and metabolome of the liver of C57BL/6 male mice treated with Rapa (14 ppm, encapsulated in the food), DR (40%), or Rapa and DR for 6 months, starting at 2 months of age (7). We show that DR and Rapa have overlapping yet distinct effects on many genes/pathways, which is not entirely surprising because it is known that DR, like Rapa, also inhibits mTOR activity and increases autophagy. More importantly, however, we observed that the combination of both treatments has a larger effect on gene expression than either treatment alone (8). However, when we measured physiological effects of the interventions, we found that while DR improved glucose tolerance as expected, mice treated with Rapa failed to show improved glucose tolerance (7). This is consistent with the literature, where chronic treatment with Rapa has been shown to lead to glucose intolerance (2).

Based on these data and taking advantage of our vast metabolome and transcriptome data sets, we attempted to discern both similarities and differences in the effects of Rapa and DR on energy metabolism and to begin identifying

the mechanism(s) of insulin resistance induced by Rapa. Our studies indicate that in contrast to DR, Rapa has no effect on pathways linked to glucose metabolism. In addition, a major difference between the two treatments was their effects on lipid metabolism: Although both treatments inhibit lipogenesis and fat storage, increasing the generation of nonesterified fatty acids (NEFAs) via activation of lipolysis, only DR—but not Rapa—induces further metabolism of these fatty acids via  $\beta$ -oxidation and production of ketone bodies.

## METHODS

### *Animals and Feeding Regiment*

Male C57BL/6 mice (4 weeks of age) were purchased from The Jackson Labs (Bar Harbor, ME). The mice were fed a mouse chow, 7012 Teklad LM-450 (Harlan Laboratories, Madison, WI) until 2 months of age, after which they were divided into four dietary regimens: ad libitum (AL), 40% DR, AL plus 14 ppm of rapamycin (Rapa), and 40% diet restriction plus 14 ppm of rapamycin (DR + Rapa). AL mice were fed a commercial mouse chow, Purina Mills Test Diet Control #1810306 (Purina Mills, St Louis, MO), without restriction. The DR mice were fed the same diet but received 40% less food than the AL fed mice. The Rapa mice were fed the AL diet with 14 ppm of encapsulated rapamycin in the food as described by Harrison and coworkers (3). DR + Rapa mice were fed a 40% DR plus 14 ppm of encapsulated rapa in the food. DR and DR + Rapa animals were fed at 3:30 in the afternoon, and the food intake data indicate there was no difference between groups AL vs. Rapa or DR vs. DR + Rapa. Mice were maintained on these dietary regimens until 8 months of age (6 months of treatment), at which time tissues were collected. All procedures followed the guidelines approved by the Institutional Animal Care and Use Committee at the University of Texas Health Science Center at San Antonio. Nonfasted mice were randomly chosen from the different groups and euthanized by carbon dioxide between 8:30 and 10:30 AM; the livers were snap frozen in liquid nitrogen and stored at  $-80^{\circ}\text{C}$  until used.

### *C2C12 Cell Culture and Sirt3 Overexpression*

Mouse muscle C2C12 myoblasts were cultured in high-glucose DMEM (Life technologies, Grand Island, NY) supplemented with 10% Hyclone fetal bovine serum, 1 mM sodium pyruvate and 100  $\mu\text{g}/\text{mL}$  penicillin–streptomycin. mSirt3-L plasmid was obtained from Addgene (Cambridge, MA) and transfected into C2C12 cells using FuGENE HD Transfection Reagent (Roche, Indianapolis, IN). Overexpression of Sirt3 was confirmed by immunoblotting (sirt3 antibody was obtained from Cell signaling; Danvers, MA).

### *Immunoblotting*

Frozen liver tissue was homogenized in ice-cold RIPA buffer (50 mM Tris–HCl pH 7.4, 1% Nonidet P-40, 1% Sodium deoxycholate, 0.15 M NaCl) supplemented with protease and phosphatase inhibitors (Roche). The supernatant was collected after centrifugation at  $4^{\circ}\text{C}$ , 12,000g for 10 minutes. Proteins were separated by sodium dodecyl sulfate–polyacrylamide gel electrophoresis followed by transfer to polyvinylidene fluoride membrane. Target proteins were detected with the following specific monoclonal or polyclonal antibodies: Actin (MP Biomedicals, Solon, OH); Car 1/2 (Santa Cruz, Dallas, TX), Insig2 (Aviva Systems Biology, San Diego, CA); Srebp1 (Novus biologicals, Littleton, CO), Cpt1 (Alpha Diagnostic, Intl Inc., San Antonio, TX); CD36 (Pierce, Rockford, IL). Images were analyzed by Imagemlab software (Bio-rad, Hercules, CA).

### *Mitochondria Isolation*

Liver tissues were homogenized in isolation buffer (250 mM mannitol, 75 mM sucrose, 0.5 mM EGTA, 0.1 mM EDTA, 10 mM HEPES, pH 7.4) and centrifuged at 600g for 10 minutes. The supernatant was centrifuged at 10,000g for 10 minutes, and the pellet was resuspended in the same buffer containing 0.5% BSA and centrifuged again to remove fat. The final pellet was resuspended in respiration buffer (10 mM Tris, pH 7.4, 250 mM sucrose, 10 mM  $\text{KH}_2\text{PO}_4$ , 1 mM EGTA) and sonicated thrice, 30 seconds each time.

### *Measurement of Palmitoyl-CoA Dehydrogenase Activity*

Palmitoyl-CoA dehydrogenase (EC: 1.3.8.8) activity was measured in mitochondrial extracts at  $32^{\circ}\text{C}$  (9). The assay medium contained 100 mM potassium phosphate buffer, pH 8.0, 40  $\mu\text{M}$  DCIP, 100  $\mu\text{M}$  FAD, 2.5 mM KCN, and 50  $\mu\text{M}$  palmitoyl-CoA (substrate). Activity was determined at 600 nm using a Beckman DU-800 spectrophotometer. Enzyme activities are presented as mean  $\pm$  SE ( $n = 4$ ) and expressed as  $\mu\text{mol}/\text{min}/\text{mg}$  protein.

### *Measurement of $\beta$ -Hydroxybutyric Dehydrogenase Activity*

$\beta$ -hydroxybutyric dehydrogenase (EC 1.1.1.30) activity assay was measured in mitochondrial extracts at  $20^{\circ}\text{C}$  (10). The assay medium contained 40 mM Tris buffer, pH 8.5, 50 mM nicotinamide, 10 mM cysteine, 2 mM NAD, 1 mM KCN, and 20 mM DL- $\beta$ -hydroxybutyrate (substrate). Activity was determined at 340 nm using a Beckman DU-800 spectrophotometer. Enzyme activities are presented as mean  $\pm$  SE ( $n = 4$ –5) and expressed as  $\mu\text{mol}/\text{min}/\text{mg}$  protein.

### Measurement of NEFAs in Serum Samples

Serum levels of NEFAs were determined by a colorimetric assay, using a kit purchased from Wako Chemicals (Richmond, VA).

### Fatty Acid Oxidation Assay Using Seahorse XF Analyzer

Palmitate–BSA conjugate stock of 1 mM palmitate: 0.17 mM BSA was prepared according to the protocol provided by Seahorse (North Billerica, MA). Mouse muscle C2C12 myoblasts were seeded at a density of 10,000 cells/well in a 24-well Seahorse microplate in high-glucose Dulbecco's Modified Eagle's medium supplemented with 10% fetal bovine serum. Cells were treated with DMSO, 2 mM metformin, or 250 nM Rapa for 24 hours (cells overexpressing Sirt-3 were used as an additional control.). Cells were then washed with 1× KHB buffer (110 mM NaCl, 4.7 mM KCl, 2 mM MgSO<sub>4</sub>, and 1.2 mM Na<sub>2</sub>HPO<sub>4</sub>, pH 7.4, 2.5 mM glucose, 0.5 mM carnitine) and incubated for 1 hour without CO<sub>2</sub>. The palmitate–BSA conjugate was injected to a final concentration of 200 μM palmitate/34 μM BSA. Extracellular oxygen consumption rate and extracellular acidification rate were measured using the seahorse XF 24 Extracellular Flux Analyzer (Seahorse biosciences, North Billerica, MA).

### Quantitative Real-Time PCR

Total RNA was extracted from frozen liver tissues (25 mg) using the RNeasy kit (Qiagen, Valencia, CA) according to the manufacturer's instructions, and DNA contamination was removed by TURBO DNase (Ambion, Inc., Foster City, CA). The RNA yield of each sample was determined spectrophotometrically, and the quality of total RNA extracted from each sample was monitored by A260:A280 ratio. One microgram of RNA was used to generate cDNA using the Retroscript kit (Ambion, Inc.). Primers were designed using Primer Express (Applied Biosystem, Inc., Foster City, CA) and Primer-BLAST (NCBI). Quantitative real-time PCR (qRT-PCR) was performed using SYBR Green PCR Master Mix (Applied Biosystem, Inc.) using actin as a housekeeping control with detection by a 7500 Real-Time

PCR Detection System (Applied Biosystem, Inc.). Analysis of the qRT-PCR results was done using the  $\Delta\Delta\text{CT}$  method.

### Metabolomics

Frozen liver tissues obtained from DR ( $N = 7$ ), DR + Rapa ( $N = 9$ ), AL ( $N = 10$ ), and Rapa ( $N = 10$ ) mice were analyzed for metabolite levels by Metabolon (Durham, NC) using gas chromatography/mass spectrometry (GC/MS) and liquid chromatography coupled with tandem mass spectrometry (LC/MS/MS) to identify metabolites using a library of more than 1,000 compounds and quantify the levels of the metabolites in the samples.

### Statistical Analysis

Unless specified, all data were expressed as mean  $\pm$  standard error of the mean (*SEM*) and were analyzed by one-way ANOVA with pairwise comparisons using Tukey's post hoc test. Statistical significance is indicated by  $p < .05$ .

For metabolomics analysis, data were normalized by Metabolon, and the statistical analysis was conducted by the Tukey's post hoc test ( $p$  value). Multiple comparisons test (false discovery analysis;  $q$  value) was conducted using R package (v 1.30.0, Dabney, A and Storey, J). Statistical significance is indicated at  $q$  value less than 0.05 and fold change greater than 15%.

## RESULTS

To compare the effects of DR and Rapa on energy metabolism, we focused first on hepatic glycogen and glucose metabolism. The data in Table 1 show that the liver of DR-treated mice has significantly lower levels of glycogen breakdown products compared with AL, suggesting that glycogen stores have been largely converted into glucose. In contrast, Rapa treatment did not alter glycogen storage, and the combined group (DR + Rapa) had levels similar to those observed in the DR group. Similarly, when we measured the levels of glucose, we found that mice on DR showed a significant decrease (20%) in glucose levels in liver compared with the AL group; however, feeding Rapa did not alter the levels of liver glucose. Again, the DR + Rapa group showed a similar decrease in glucose as

Table 1. Glycogen Breakdown Metabolites

Glycogen Breakdown Products	DR	Rapa	DR + Rapa
	AL	AL	AL
Maltose	0.46* ( $p = .01$ ; $q = .01$ )	1.05 ( $p = .7$ ; $q = .69$ )	0.60* ( $p = .05$ ; $q = .079$ )
Maltotriose	0.42* ( $p = .019$ ; $q = .01$ )	1.11 ( $p = .24$ ; $q = .51$ )	0.40* ( $p = .01$ ; $q = .003$ )
Maltotetraose	0.37* ( $p = .008$ ; $q = .0007$ )	1.09 ( $p = .49$ ; $q = .65$ )	0.30* ( $p = .0002$ ; $q = .0012$ )
Maltopentaose	0.25* ( $p = .001$ ; $q = .0007$ )	1.01 ( $p = .97$ ; $q = .76$ )	0.12* ( $p = .0002$ ; $q = .0012$ )
Maltohexaose	0.30* ( $p = .004$ ; $q = .018$ )	1.02 ( $p = .95$ ; $q = 0.76$ )	0.22* ( $p = .0019$ ; $q = .004$ )

Notes: AL = ad libitum; DR = dietary restriction; Rapa = rapamycin. Levels of several glycogen breakdown products were measured by The Metabolome. The data were obtained from 7 to 11 mice per group and expressed as mean  $\pm$  SD. Data were analyzed using unpaired  $t$  test with Welch's correction; the data are represented relative to AL, and the statistical significance ( $p$ ) and false discovery rates ( $q$ ) values are given in parenthesis. Asterisks denote those values that are significantly different ( $p \leq .05$ ) from AL mice.

observed in the DR mice (Figure 1A). These results do not reflect differences in fasting at the time of sacrifice (morning) because blood glucose levels and stomach weights showed no significant differences between the DR, AL, and Rapa mice (Supplementary Figure 1). To determine whether the decrease in glucose levels is due to further intrahepatic metabolism, we measured the levels of two key metabolic intermediaries: glucose 6-phosphate and lactate. The data in Figure 1B and C show that both of these metabolites are significantly lower (43% and 30%, respectively) in DR. None of these metabolites were significantly altered by Rapa feeding alone, and the DR + Rapa group was similar to the DR group.

Our data also suggest that in response to DR there is an increase in shunting of glucose-6-phosphate into the pentose phosphate pathway because the levels of 6-phosphogluconate are significantly higher in the DR group (Figure 1D). This may explain why, in spite of having high glucose metabolism, the DR treated mice show no significant changes in metabolites in the tri carboxylic acid cycle (Supplementary Figure 2).

To gain insight into why Rapa-treated mice become glucose and insulin intolerant, we measured the other metabolic branch that has a major impact on glucose metabolism and lipid metabolism. Preliminary evidence obtained from our microarray analysis showed that both DR and Rapa significantly decreased the transcripts of the *Srebp-1* transcription factor, a lipogenesis inducer, as well increased levels of *Insig 1* and *2* transcripts, which are inhibitors of *Srebp-1* (11). These data were corroborated by qRT-PCR and by western blot analysis as shown in Figure 2A and B and suggest that both DR and Rapa have a similar effect in inhibiting lipid storage. In addition to reducing lipid storage, our qRT-PCR data also suggest that lipolysis is increased in both the DR and Rapa groups. For example, adipose triglyceride lipase (ATGL), hormone-sensitive lipase (HSL), and monoacylglyceride lipase (MGL) are significantly increased in DR, Rapa, and DR + Rapa groups (Supplementary Figure 3), which is in accordance with previous studies in mice and humans, showing that DR increased the expression of these enzymes (12,13). We also measured the levels of NEFAs and glycerol. All groups show increased levels of NEFAs compared with AL-fed mice although the DR + Rapa group did not reach significance ( $p = .052$ ; Figure 2C). We did not observe any significant change in serum glycerol between the three groups and mice fed AL (Supplementary Figure 4).

The DR and Rapa mice differ significantly in their effect on another aspect of lipid metabolism: fatty acid oxidation. DR, but not Rapa, increases the transcript levels and protein of the constitutive androstane receptor (CAR), an orphan nuclear receptor that has been reported to activate mitochondrial fatty acid  $\beta$ -oxidation, as well as improve insulin sensitivity and glucose utilization by the liver (14) (Figure 3A). Consistent with this result, we found significantly lower levels of several long-chain fatty acid metabolites, which

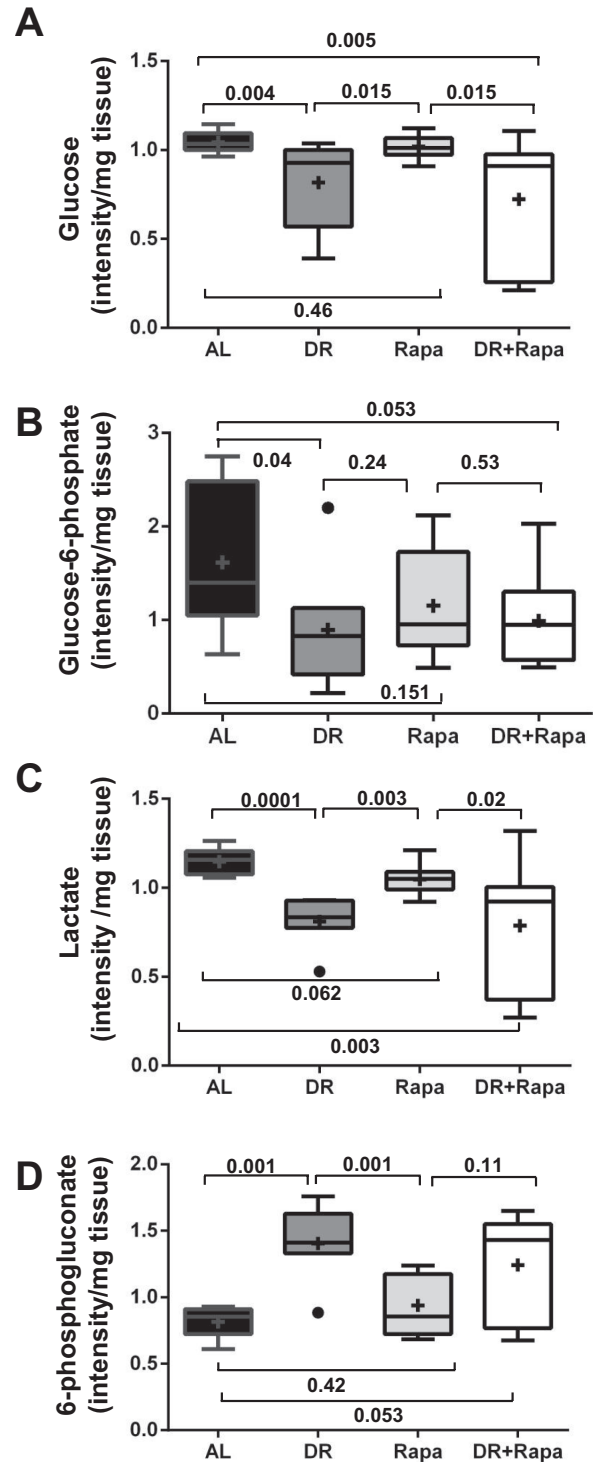


Figure 1. Dietary restriction (DR) but not rapamycin increases glycogen breakdown and glucose metabolism. Levels of glucose (A), glucose 6-phosphate (B), lactate (C), and 6-phosphogluconate (D) were determined in mice fed for 6 months of treatment (starting at 2 months of age) under AL (solid bars), DR (grey bars), Rapa (light grey), and DR + Rapa (open bars). Each metabolite was measured by Metabolon, and the data were obtained from 7–11 mice per group and expressed as mean  $\pm$  SD using a box and whisker plot, where the plus symbol (+) represents the average, and black dots (•) represent the outliers. Data were analyzed by one-way ANOVA with Tukey’s post hoc test. Specific  $p$  values are denoted in the figure.

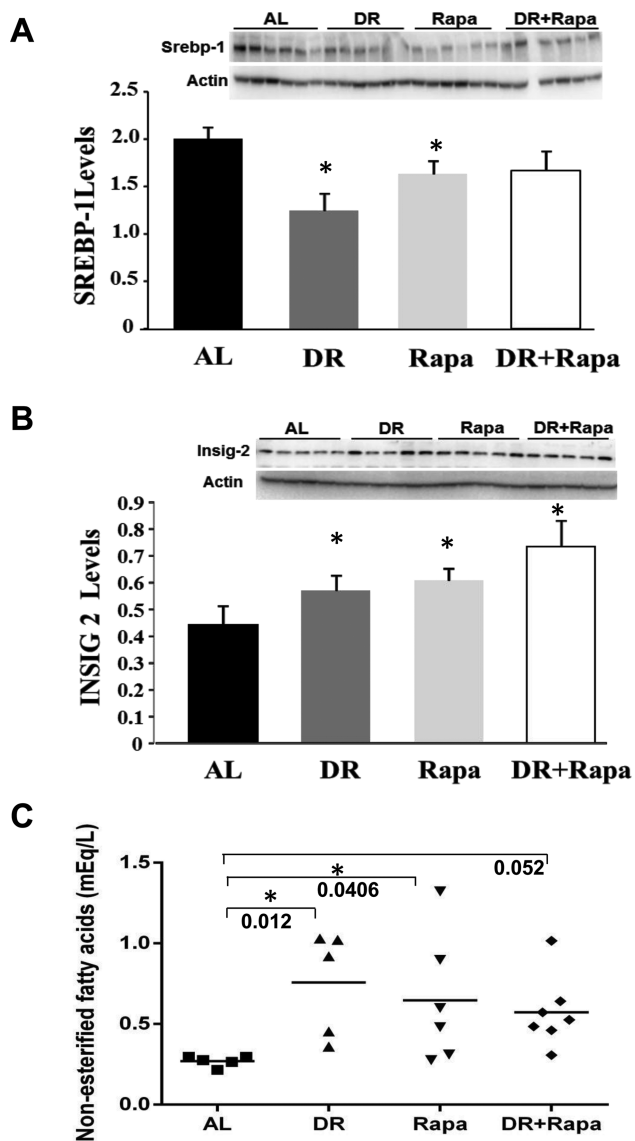


Figure 2. Both dietary restriction (DR) and rapamycin reduced expression of genes that inhibit fat storage and increased lipolysis. Lipolysis was assessed in liver samples by measuring the levels of transcription factor SREBP-1 (A), the levels of INSIG2 (B), and by the serum levels of nonesterified fatty acids (NEFAs; C). A representative western blot for Srebp-1 and Insig2 measurements is shown next to the respective quantification. The data were obtained from 5 to 6 mice per group: AL (solid bars), DR (grey bars), Rapa (light grey bars), and DR + Rapa (open bars). The data were expressed as mean  $\pm$  SEM and analyzed using one-way ANOVA with the Tukey's post hoc test; asterisk denotes those values that are significantly different from AL mice at the  $p \leq .05$  level. Specific  $p$  values are denoted in Figure 2C.

are a signature of  $\beta$ -oxidation in the livers of DR mice but not Rapa-treated mice (Table 2). These data suggest the lipids produced by DR-induced lipolysis are effectively metabolized via fatty acid  $\beta$ -oxidation in the DR mice. In contrast, Rapa treatment decreases lipid synthesis and increases NEFAs without inducing an increase in fatty acid  $\beta$ -oxidation, thereby increasing lipid accumulation.

To test whether fatty acid  $\beta$ -oxidation is activated by DR but not Rapa treatment, we measured the activity of

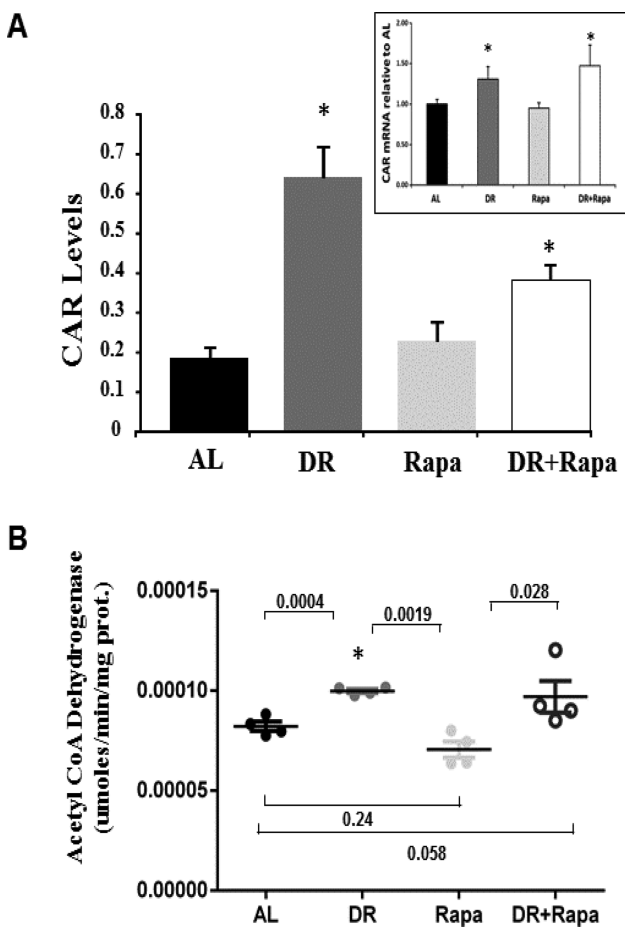


Figure 3. Dietary restriction (DR) but not rapamycin activates fatty acid  $\beta$ -oxidation.  $\beta$ -oxidation was measured by the levels of the nuclear receptor constitutive androstane receptor (CAR; A) and the activity of acetyl CoA dehydrogenase (B). The data were obtained from 4 to 6 mice per group for AL (solid symbols/bars), DR (grey symbols/bars), Rapa (light grey symbols/bars), and DR + Rapa (open symbols/bars) mice. The insert in Figure 3A represents the qPCR data for CAR transcript. The data in Figure 3A are expressed as mean  $\pm$  SEM, and data in Figure 3B are expressed as mean  $\pm$  SD. Both set of data were analyzed using one-way ANOVA; asterisks denote those values that are significantly different ( $p \leq .05$ ) from AL and DR mice, respectively. The solid line in the scatter plot (Figure 3B) represents the mean. Specific  $p$  values are denoted in the figure.

long-chain acetyl CoA dehydrogenase, one of key enzymes in the fatty acid  $\beta$ -oxidation pathway using mitochondrial liver extracts with palmityl CoA as a substrate. Figure 3B shows that the long-chain acetyl CoA dehydrogenase activity is significantly higher (20%) in the DR mice compared with AL mice. However, Rapa treatment failed to activate long-chain acetyl CoA dehydrogenase. Although the combined treatment showed a tendency similar to DR, the mouse to mouse variation was high, and the DR + Rapa group was not quite statistically different from AL group ( $p = .058$ ).

Acetyl CoA obtained from  $\beta$ -oxidation can be utilized in the tri carboxylic acid cycle, but tri carboxylic acid intermediaries were not affected by either DR or Rapa. Similarly, acetyl CoA does not seem to be utilized for fatty acid

Table 2. Metabolites From Long-Chain Fatty Acids

Long-Chain Fatty Acids	DR	Rapa	DR + Rapa
	AL	AL	AL
Myristate (14:0)	0.74 ( $p = .3$ ; $q = .17$ )	0.86 ( $p = .58$ ; $q = .69$ )	0.87 ( $p = .63$ ; $q = .17$ )
Myristoleate (14:1n5)	0.86 ( $p = .65$ ; $q = .16$ )	0.73 ( $p = .41$ ; $q = .61$ )	0.95 ( $p = .68$ ; $q = .22$ )
Pentadecanoate (15:0)	0.80 ( $p = .3$ ; $q = .17$ )	0.95 ( $p = .79$ ; $q = .74$ )	0.75 ( $p = .10$ ; $q = .05$ )
Palmitate (16:0)	0.77 ( $p = .08$ ; $q = .07$ )	0.98 ( $p = .86$ ; $q = .75$ )	0.76 ( $p = .16$ ; $q = .07$ )
Palmitoleate (16:1n7)	0.45 ( $p = .03$ ; $q = .004$ )*	0.85 ( $p = .6$ ; $q = .69$ )	0.58 ( $p = .17$ ; $q = .08$ )
Margarate (17:0)	0.64 ( $p = .02$ ; $q = .01$ )*	1.09 ( $p = .6$ ; $q = .7$ )	0.71 ( $p = .17$ ; $q = .07$ )
10-Heptadecenoate (17:1n7)	0.39 ( $p = .002$ ; $q = .006$ )*	0.92 ( $p = .69$ ; $q = .7$ )	0.50 ( $p = .04$ ; $q = .02$ )*
Stearate (18:0)	0.91 ( $p = .37$ ; $q = .11$ )	1.05 ( $p = .59$ ; $q = .69$ )	0.90 ( $p = .4$ ; $q = .16$ )
Oleate (18:1n9)	0.48 ( $p = .16$ ; $q = .11$ )	0.78 ( $p = .58$ ; $q = .69$ )	0.57 ( $p = 0.32$ ; $q = 0.11$ )
<i>cis</i> -Vaccenate (18:1n7)	0.28 ( $p = .04$ ; $q = .06$ )*	0.72 ( $p = .48$ ; $q = .64$ )	0.50 ( $p = .22$ ; $q = .09$ )
Stearidonate (18:4n3)	0.38 ( $p = .04$ ; $q = .04$ )*	0.73 ( $p = .36$ ; $q = .58$ )	0.41 ( $p = .05$ ; $q = .04$ )*
Nonadecanoate (19:0)	0.60 ( $p = .02$ ; $q = .003$ )*	1.17 ( $p = .36$ ; $q = .58$ )	0.63 ( $p = .05$ ; $q = .03$ )*
10-Nonadecenoate (19:1n9)	0.50 ( $p = .14$ ; $q = .08$ )	0.90 ( $p = .8$ ; $q = .74$ )	0.62 ( $p = .32$ ; $q = .11$ )
Eicosenoate (20:1n9 or 11)	0.45 ( $p = .04$ ; $q = .05$ )*	1.08 ( $p = .8$ ; $q = .74$ )	0.64 ( $p = .38$ ; $q = .12$ )
Dihomo-linoleate (20:2n6)	0.57 ( $p = .03$ ; $q = .06$ )*	1.05 ( $p = .87$ ; $q = .75$ )	0.68 ( $p = .24$ ; $q = .10$ )
Mead acid (20:3n9)	0.70 ( $p = .08$ ; $q = .033$ )	0.69 ( $p = .07$ ; $q = .47$ )	0.69 ( $p = .07$ ; $q = .04$ )
Arachidonate (20:4n6)	0.94 ( $p = .5$ ; $q = .32$ )	0.92 ( $p = .45$ ; $q = .63$ )	1.04 ( $p = .74$ ; $q = .19$ )
Docosadienoate (22:2n6)	0.57 ( $p = .01$ ; $q = .02$ )*	1.15 ( $p = .34$ ; $q = .69$ )	0.81 ( $p = .63$ ; $q = .17$ )
Docosatrienoate (22:3n3)	0.75 ( $p = .39$ ; $q = .29$ )	0.87 ( $p = .67$ ; $q = .7$ )	0.73 ( $p = .34$ ; $q = .11$ )
Adrenate (22:4n6)	1.09 ( $p = .7$ ; $q = .35$ )	1.07 ( $p = .68$ ; $q = .7$ )	1.11 ( $p = .75$ ; $q = .2$ )

Notes: AL = ad libitum; DR = dietary restriction; Rapa = rapamycin. Levels of several fatty acid breakdown products (long-chain fatty acids) were measured by The Metabolome. The data were obtained from 7 to 11 mice per group and expressed as mean  $\pm$  SD. Data were analyzed using unpaired *t* test with Welch's correction; the data are represented relative to AL, and the *p* and *q* values are given in parenthesis. Asterisks denote those values that are significantly different ( $p \leq .05$ ) from AL mice.

biosynthesis because the synthesis of fatty acids is inhibited by both treatments. An alternative pathway is that acetyl CoA could be used to generate ketone bodies. Therefore, we measured the levels of the ketone body of 3-hydroxybutyrate in liver tissue from the four groups of mice. The data in Figure 4A show that DR, but not Rapa, leads to significantly higher levels of 3-hydroxybutyrate compared with the AL and control group. The DR + Rapa mice had levels of 3-hydroxybutyrate similar to the DR group. To identify whether this is due to a direct effect on the ketogenesis pathway, we measured the activity of the rate-limiting enzyme in the generation of ketone bodies,  $\beta$ -hydroxybutyrate dehydrogenase. Our data show that the activity of  $\beta$ -hydroxybutyrate dehydrogenase is significantly increased in both the DR and DR + Rapa groups compared with the AL group. Rapa had no effect on  $\beta$ -hydroxybutyrate dehydrogenase activity.

Control of fatty acid metabolism is also regulated by the uptake of fatty acids by transporters (15), and this upregulation is partially due to increased gene expression (16). To assess this aspect of fatty acid metabolism under these treatments, we measured the levels of mRNAs for several transporters that showed significant changes in our previously published microarray data: *Cd36*, a transporter that mobilizes long-chain fatty acids into the cell; *Octn2* and *mCac*, mitochondrial transporters for fatty acids; and *Cpt-1*, the rate-limiting transporter for the overall  $\beta$ -oxidation pathway (17). The levels of all of these transcripts were reduced by Rapa, but not reduced by DR. Immunoblot

analysis showed that DR significantly increased the expression of *Cd36* (Figure 5A), and the levels of *CPT1* were higher in both the DR and Rapa groups, a result that was inconsistent with the microarray analysis of transcripts (Figure 5B).

Our data showed that combined treatment by DR and Rapa mitigates glucose intolerance and insulin insensitivity compared with treatment by Rapa alone (Supplementary Figure 5), suggesting that short-term DR (6 months) can counteract the effect of Rapa on insulin insensitivity. We next attempted to test whether  $\beta$ -oxidation could be reactivated pharmacologically in the presence of Rapa. To test this hypothesis, we measured  $\beta$ -oxidation in C2C12 myoblasts because it has been shown that insulin insensitivity induced by Rapa can be mimicked in these cells (18), and we treated the cells with metformin (Met) because Dhahbi and coworkers (19) showed that treating mice for 8 weeks with Met produced a transcriptional profile in liver resembling DR. As shown in Figure 6A, C2C12 myoblasts showed an increased oxygen consumption rate in the presence of palmitate-BSA, a measure of  $\beta$ -oxidation, and this effect was enhanced when cells were treated with Met or by overexpressing *Sirt3* protein, two manipulations that are known to activate  $\beta$ -oxidation (20,21). However, this effect in  $\beta$ -oxidation was not induced when cells were incubated with Rapa alone (Figure 6A). However, when Met was combined with Rapa, fatty acid  $\beta$ -oxidation was restored in spite of the presence of Rapa (Figure 6B).

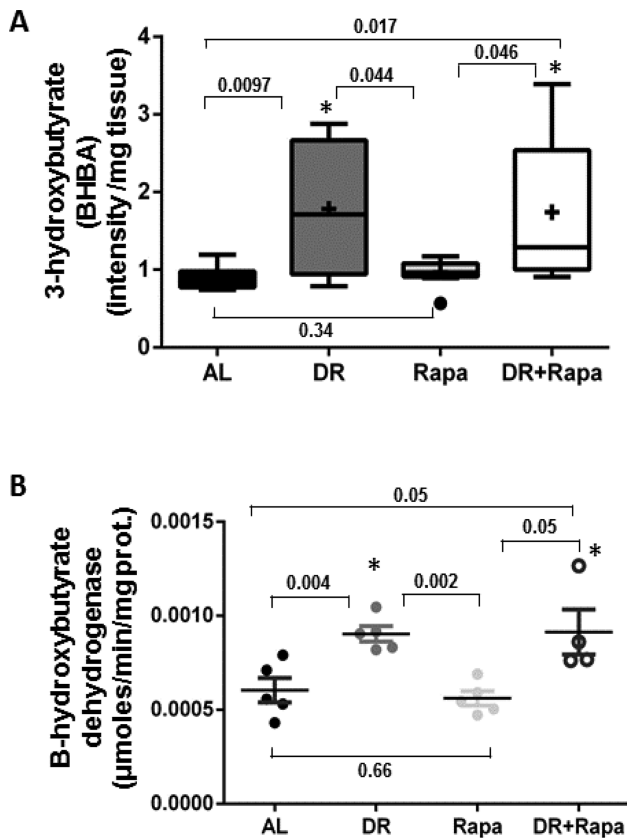


Figure 4. Dietary restriction (DR) but not rapamycin activates ketogenesis pathway. Ketogenesis was determined by the level of 3-hydroxybutyrate (BHBA; A) and by the enzymatic activity of  $\beta$ -hydroxybutyrate dehydrogenase (B). The data were obtained from 5 to 11 mice per group, AL (solid symbols/bars), DR (grey symbols/bars), Rapa (light grey symbols/bars), and DR + Rapa (open symbols/bars). The data are expressed as mean  $\pm$  SD and analyzed by one-way ANOVA with Tukey's post hoc test. The asterisk denotes those values that are significantly different from AL mice at the  $p \leq .05$  level (specific  $p$  values are denoted in the figure). The solid line in the scatter plot (Figure 4B) represents the mean.

## DISCUSSION

Both Rapa and DR produce a significant increase in mouse life span, and both interventions have similar effects on several intracellular signaling pathways including inhibition of mTOR (3), activation of autophagy (22), and increased resistance to induction of cellular senescence (23). However, they have opposite effect on glucose and insulin sensitivity: while DR increases insulin sensitivity (24), Rapa leads to insulin resistance (2). Therefore, while feeding mice Rapa leads to an increase in life span and several aspects of health span, the negative effects of rapamycin on insulin sensitivity significantly decrease its translational potential.

Although our data showing decreased insulin sensitivity is consistent with several previous reports (25–27), a study by Fang and coworkers (28) showed that mice treated with Rapa for 20 weeks had increased insulin sensitivity. More recently, Miller and coworkers (29) have shown that in genetically heterogeneous mice (UM-HET3), the glucose intolerance induced by Rapa is also dose dependent. We think that the discrepancy with the data from Fang may be explained by differences in administration route. Indeed, Fang's group delivered the drug by i.p. injection every other day, whereas we delivered Rapa encapsulated in the food (AL). This difference in administration route could be quite important because the half-life of Rapa in mice is  $\sim$ 6 hours (30). However, we think that the most important difference is that Fang and coworkers did all their metabolic measurements in fasted mice (fasted for 16 hours), which may activate other pathways, for example, AMPK, leading to increased activity of fatty acid oxidation and ketogenesis pathways. In our study, we did not fast the animals to avoid these DR-like effects on metabolism.

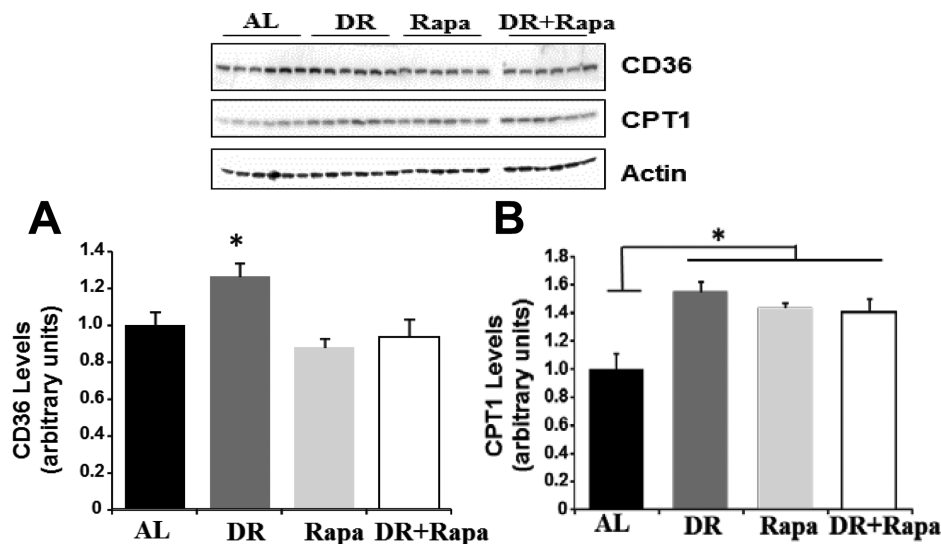


Figure 5. The fatty acid transporter, CD36, is overexpressed by dietary restriction (DR) but not by rapamycin. Levels of fatty acid transporters CD36 (A) and CPT-1 (B) were measured in the whole liver homogenate obtained from six mice per group: AL (solid bars), DR (grey bars), Rapa (light grey bars), and DR + Rapa (open bars). A representative western blot for CD36 and CPT-1 measurements is shown next to the respective quantification. The data are expressed as mean  $\pm$  SEM and analyzed using one-way ANOVA with the Tukey's post hoc test; asterisk denotes those values that are significantly different from AL mice at the  $p \leq .05$  level.

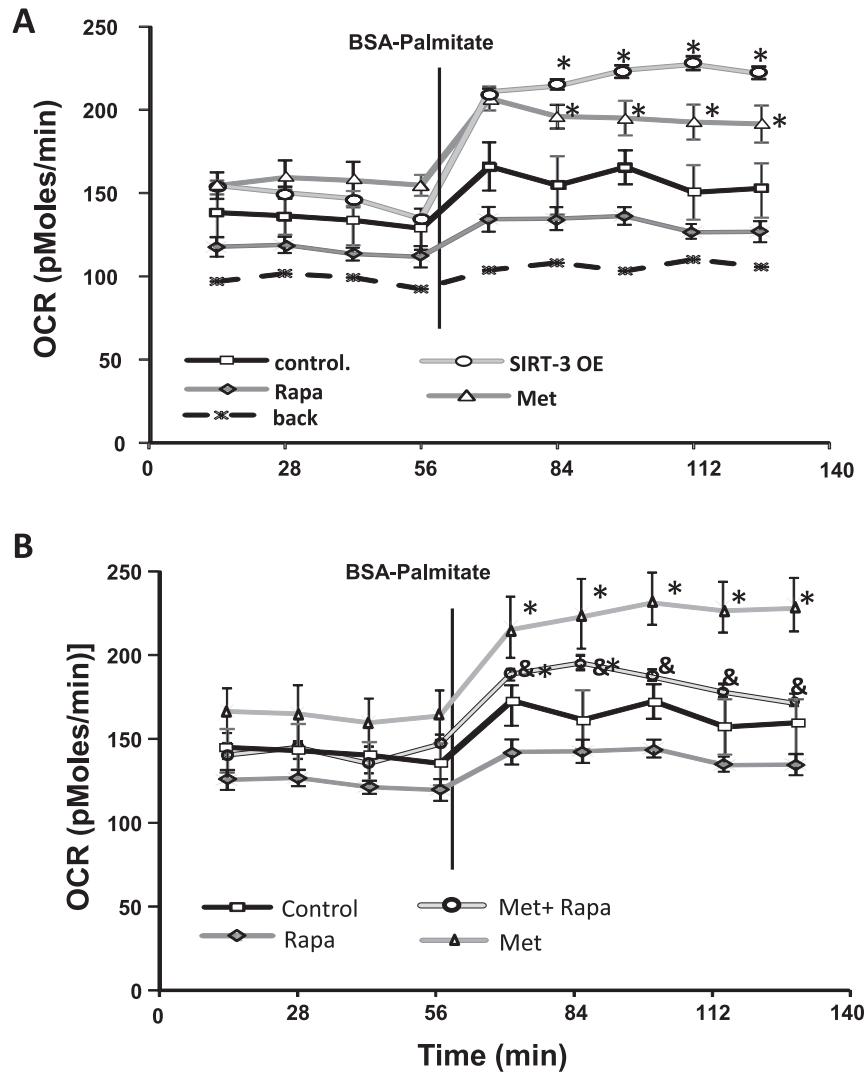


Figure 6. The repressed fatty acid  $\beta$ -oxidation induced by rapamycin is rescue in vitro by metformin. Fatty acid  $\beta$ -oxidation was determined by Seahorse analysis using C2C12 cells treated with BSA-palmitate and measuring the oxygen consumption rate (OCR) under the following conditions: (A) Control (squares), Rapa 250 nM (diamonds), metformin 2 mM (triangles), and SIRT3 overexpression (circles). BSA alone was used as negative control (dashed line). (B) Effect of a combined treatment of metformin plus rapamycin (circles) on fatty acid  $\beta$ -oxidation. The data are expressed as the mean  $\pm$  SEM and analyzed by one-way ANOVA. Asterisks denote those values that are significantly different from controls, and ampersands (&) denote those values different from rapamycin alone ( $p \leq .05$ ).

The purpose of this study was to identify the underlying cause behind the contrasting effect of DR and Rapa on insulin sensitivity; therefore, we focused our study on metabolism in the liver, the main tissue involved in metabolic responses to changes in nutritional status (31). Our first attempt was to compare glycogen storage and glucose metabolism. Although our array and metabolomics data confirmed previous reports on the effect of DR on glucose metabolism (32,33), we found that Rapa treatment does not affect either glycogen breakdown or glucose metabolism, thus indicating that this was not the mechanism mediating insulin resistance induced by Rapa. Higher levels of 6-phosphogluconate suggest that DR may induce further metabolism of glucose through the pentose phosphate pathway (Figure 1). Although this is a steady-state measurement

and may not represent the rate of flux through the pathway, this is consistent with studies in plants where an increase in 6-phosphogluconate was correlated with increased activity of the pentose phosphate pathway (34). Moreover, metabolomics analysis of plasma from monkeys showed higher levels of gluconate and acetate in animals under DR, suggesting an increased metabolic flux through the pentose phosphate pathway (35). These changes in metabolism should lead to an increase in NADPH production, which could explain the more reduced redox state (GSH/GSSG ratio) observed in DR mice but not in Rapa-treated mice (7).

The role of alterations in lipid metabolism on glucose metabolism and insulin resistance is well established. For example, increased plasma-free fatty acid concentrations

are typically associated with impaired insulin-mediated glucose uptake (36), and acute elevation in plasma-free fatty acid concentrations for 5 hours induced insulin resistance in a rat model, as reflected by a ~35% reduction in the glucose infusion rate during an hyperinsulinemic–euglycemic clamp (37).

Our data show that both DR and Rapa lead to increased production of NEFAs, leading to changes in the lipid composition of plasma, indicating that both DR and Rapa lead to changes in lipid metabolism consistent with decreased fat storage and increased lipolysis (Figure 2). Although we did not find major changes in serum glycerol levels, this is in accordance with previous data where glycerol levels under DR are maintained constant (38). This is important because although activation of lipid breakdown and utilization of fatty acids are appropriate responses to DR (because of reduced availability of nutrients), a similar response to Rapa under ad-lib condition could lead to accumulation of plasma lipids (dyslipidemia) and enhanced insulin insensitivity, as observed in animals treated with Rapa alone.

Our data are supported by studies in mice and in human patients treated with Rapa, both of whom show elevated circulating levels of NEFAs and triglycerides (39). Furthermore, Sirulimus (a rapalog) increases the expression of *insig-1* and decreases expression of *srebp-1* both in vascular smooth muscular cells and in hepatocytes (HepG2) (40,41). Using 3T3-L1 differentiated adipocytes treated with Rapa, Soliman and coworkers showed a 50% reduction in insulin-stimulated triglycerides storage and increased lipolysis (12). Thus, our data are consistent with the available literature, in animal models, in cells in culture, and in humans, and which suggest a common molecular mechanism associated with Rapa-induced dyslipidemia.

A surprising outcome of our study was to discover that, although both treatments have a similar effect on synthesis and degradation of lipids, DR, but not Rapa, provokes an induction of  $\beta$ -oxidation. It is noteworthy that only DR leads to increased levels of CAR, which was originally identified as essential for the xenobiotic response, but more recently it has been implicated in regulation of glucose and lipid metabolism. Indeed, activation of CAR improves

glucose uptake and utilization by the liver, and it activates fatty acid oxidation in the mitochondria (42). Using COS7 cells, Jingami's group demonstrated that the activation of CAR is mediated by PGC-1 $\alpha$ , which interacts with CAR through its serine/arginine-rich domain (43), which is consistent with our preliminary experiments which show that the levels of PGC-1 $\alpha$  transcript are elevated by DR but not Rapa (data not shown). Thus, it is possible that PGC-1 $\alpha$  and the nuclear receptor CAR work together to regulate genes involved in nutrient and xenobiotic transport, metabolism, and stress resistance by DR (44).

Animals treated with Rapa alone fail to activate the ketogenesis pathway. This could be a direct effect of Rapa on the rate-limiting enzymes in the ketogenesis pathway such as  $\beta$ -hydroxybutyrate dehydrogenase, but it could also be an indirect effect. For example, if glucagon is not activated by Rapa, then ketogenesis may not be initiated. Alternatively, if the main energy consumers, like brain and skeletal muscle, do not require additional energy under *ad libitum* feeding with Rapa, these tissues may generate a negative feedback to the hepatic ketogenesis pathway. The results reported here do not test these hypotheses; however, our lab is currently pursuing experiments to assess these explanations.

Our data also indicate that Rapa affects the levels of fatty acid transporters. Although our microarray data suggest that gene expression of most fatty acid transporters is reduced in the presence of Rapa, western blot data showed that FAT/CD36 transporter was significantly increased by DR and suggested that protein levels of FAT/CD36 were reduced under Rapa treatment (did not reach significance  $p = .17$ ). This may have some relevance because experiments using genetically modified rodents have identified a clear role for CD36 in fatty acid and glucose metabolism (45). For example, a deletion variant in *Cd36* was detected in the spontaneous hypertensive rats (SHR/NIH strain) that was linked to the transmission of insulin resistance and disordered fatty acid metabolism (46). Thus, it appears that in addition to the negative effects on  $\beta$ -oxidation/ketogenesis, Rapa may also alter the rate of lipid transport inside the cell and/or into the mitochondria. Clearly, this hypothesis requires further corroboration, but our data suggest a possible mechanism to explain the observed increase in dyslipidemia under Rapa treatment.

Mice fed Rapa alone do not activate  $\beta$ -oxidation; however,  $\beta$ -oxidation can be activated *in vitro* in the presence of metformin. It is well known that metformin activates the AMPK signaling pathway, which has been previously associated with enhanced  $\beta$ -oxidation. Metformin-treated mice have been shown to have a transcriptional profile resembling DR (19), and metformin is currently the drug of choice to improve insulin sensitivity and promote fatty acid usage in diabetic patients (21). Thus, the lack of activation of  $\beta$ -oxidation by Rapa may be bypassed by the Met-mediated activation of the AMPK pathway, suggesting Rapa-induced

Table 3. Summary of the Metabolic Effects Observed in DR and Rapa Treatment

Metabolic Pathway	DR	Rapa	DR + Rapa
Glycogen breakdown	+	-	+
Glucose metabolism	++	-	+
Fat storage	+	+	+
$\beta$ -oxidation	++	-	+
Ketogenesis	++	-	+

Notes: DR = dietary restriction; Rapa = rapamycin. The effect of DR and Rapa in each metabolic pathway is represented by a plus (+) or a minus sign (-), depending whether the pathway was or not significantly changed relative to AL control mice.

dyslipidemia and insulin resistant are not irreversible and can be addressed pharmacologically. In fact, Salmon and coworkers have shown that the negative effect of Rapa on insulin resistance can also be reversed simply by withdrawing the drug (Dr. Salmon, personal communication). Our results suggest that the addition of metformin to Rapa treatment may provide a therapeutic path to treat both insulin resistant and dyslipidemia induced by long-term treatment with Rapa.

On the other hand, Lamming and coworkers (2012) proposed, using rictor KO mice, that insulin resistance is due to an alteration in the insulin pathway by inhibition of mTORC2. Although not mutually exclusive with this interpretation, our data suggest that an imbalance in lipid metabolism may play an important role in the development of insulin resistance, and in fact, this may exacerbate the insulin resistance induced by mTORC2 inhibition. This is in agreement with previous data from Baur's lab, where Rapa increased triglycerides and reduced PGC1 $\alpha$  and mitochondrial function, all mediated by inhibition of mTORC1 (18). Furthermore, Rapa exerts its inhibitory activity of TOR complexes via binding to FKBP12 and other FKBP. Recent data indicate that depending on how much rapamycin binds to these binding proteins, the inhibitory effect on mTORC1/mTORC2 might be different (Dr. Brian Kennedy, personal communication). Therefore, Rapa treatment in vivo in wild-type mice could have different effects from those observed by using genetic inhibition/disruption of subunits of mTORC1/mTORC2.

In summary (Table 3), while DR and Rapa have a similar effect on lipolysis and fat storage, only DR activates the entire process of fatty acid metabolism, including the activation of  $\beta$ -oxidation and ketogenesis. Rapamycin's inability to activate fatty acid  $\beta$ -oxidation and ketogenesis in mice could generate an imbalance resulting in the accumulation of NEFAs, which may play a role in the development of insulin resistance. Activation of fatty acid  $\beta$ -oxidation by either DR or metformin corrects this imbalance and might lead to improved insulin sensitivity in animals treated with rapamycin. Our laboratory is currently testing these hypotheses; if proven true, then combined use of metformin and rapamycin for treating aging and age-associated diseases in humans may be possible.

#### SUPPLEMENTARY MATERIAL

Supplementary material can be found at: <http://biomedgerontology.oxfordjournals.org/>.

#### FUNDING

Financial support was provided by National Institutional of Health (NIH) RC2 Grand Opportunity grant (AG036613 to A.R.), The San Antonio Nathan Shock Aging Center (1P30-AG-13319 to A.R.), NIH T32 Training Grant (AG021890 to W.F.), and The Ellison Medical Foundation (V.I.P.), and start-up funds from the Department of Biochemistry and Biophysics and The Linus Pauling Institute (V.I.P.).

#### ACKNOWLEDGMENT

We thank Dr. Kathleen Fisher and Dr. Arlan Richardson for critical reading of this manuscript.

#### REFERENCES

- Stanfel MN, Shamieh LS, Kaeberlein M, Kennedy BK. The TOR pathway comes of age. *Biochim Biophys Acta*. 2009;1790:1067–1074. doi:10.1016/j.bbagen.2009.06.007
- Lamming DW, Ye L, Katajisto P, et al. Rapamycin-induced insulin resistance is mediated by mTORC2 loss and uncoupled from longevity. *Science*. 2012;335:1638–1643. doi:10.1126/science.1215135
- Harrison DE, Strong R, Sharp ZD, et al. Rapamycin fed late in life extends lifespan in genetically heterogeneous mice. *Nature*. 2009;460:392–395. doi:10.1038/nature08221
- Wilkinson JE, Burmeister L, Brooks SV, et al. Rapamycin slows aging in mice. *Aging Cell*. 2012;11:675–682. doi:10.1111/j.1474-9726.2012.00832.x
- Zhang Y, Bokov A, Gelfond J, et al. Rapamycin extends life and health in C57BL/6 mice. *J Gerontol A Biol Sci Med Sci*. 2013;69:119–130. doi:10.1093/gerona/glt056
- Neff F, Flores-Dominguez D, Ryan DP, et al. Rapamycin extends murine lifespan but has limited effects on aging. *J Clin Invest*. 2013;123:3272–3291. doi:10.1172/JCI67674
- Fok WC, Zhang Y, Salmon AB, et al. Short-term treatment with rapamycin and dietary restriction have overlapping and distinctive effects in young mice. *J Gerontol A Biol Sci Med Sci*. 2013;68:108–116. doi:10.1093/gerona/gls127
- Fok WC, Bokov A, Gelfond J, et al. Combined treatment of rapamycin and dietary restriction has a larger effect on the transcriptome and metabolome of liver. *Aging Cell*. 2014;13:311–319. doi:10.1111/ace1.12175
- Ikeda Y, Okamura-Ikeda K, Tanaka K. Purification and characterization of short-chain, medium-chain, and long-chain acyl-CoA dehydrogenases from rat liver mitochondria. Isolation of the holo- and apoenzymes and conversion of the apoenzyme to the holoenzyme. *J Biol Chem*. 1985;260:1311–1325. PMID:3968063
- Lehninger AL, Sudduth HC, Wise JB. D-beta-Hydroxybutyric dehydrogenase of mitochondria. *J Biol Chem*. 1960;235:2450–2455. PMID:14415394
- Yahagi N, Shimano H, Hasty AH, et al. Absence of sterol regulatory element-binding protein-1 (SREBP-1) ameliorates fatty livers but not obesity or insulin resistance in Lep(ob)/Lep(ob) mice. *J Biol Chem*. 2002;277:19353–19357. doi:10.1074/jbc.M201584200
- Soliman GA, Acosta-Jaquez HA, Fingar DC. mTORC1 inhibition via rapamycin promotes triacylglycerol lipolysis and release of free fatty acids in 3T3-L1 adipocytes. *Lipids*. 2010;45:1089–1100. doi:10.1007/s11745-010-3488-y
- Morrisett JD, Abdel-Fattah G, Hoogveen R, et al. Effects of sirolimus on plasma lipids, lipoprotein levels, and fatty acid metabolism in renal transplant patients. *J Lipid Res*. 2002;43:1170–1180. PMID:12177161
- Dong B, Saha PK, Huang W, et al. Activation of nuclear receptor CAR ameliorates diabetes and fatty liver disease. *Proc Natl Acad Sci USA*. 2009;106:18831–18836. doi:10.1073/pnas.0909731106
- Bonen A, Dyck DJ, Ibrahim A, Abumrad NA. Muscle contractile activity increases fatty acid metabolism and transport and FAT/CD36. *Am J Physiol*. 1999;276(4 Pt 1):E642–E649. PMID:10198299
- Hood DA. Invited Review: contractile activity-induced mitochondrial biogenesis in skeletal muscle. *J Appl Physiol (1985)*. 2001;90:1137–1157. PMID:11181630
- Longo N, Amat di San Filippo C, Pasquali M. Disorders of carnitine transport and the carnitine cycle. *Am J Med Genet C Semin Med Genet*. 2006. 142C(2): 77–85. doi:10.1002/ajmg.c.30087
- Ye L, Varamini B, Lamming DW, Sabatini DM, Baur JA. Rapamycin has a biphasic effect on insulin sensitivity in C2C12 myotubes due

- to sequential disruption of mTORC1 and mTORC2. *Front Genet.* 2012;3:177. doi:10.3389/fgene.2012.00177
19. Dhahbi JM, Mote PL, Fahy GM, Spindler SR. Identification of potential caloric restriction mimetics by microarray profiling. *Physiol Genomics.* 2005;23:343–350. doi:10.1152/physiolgenomics.00069.2005
  20. Hirschey MD, Shimazu T, Goetzman E, et al. SIRT3 regulates mitochondrial fatty-acid oxidation by reversible enzyme deacetylation. *Nature.* 2010;464:121–125. doi:10.1038/nature08778
  21. Smith DL Jr, Elam CF Jr, Mattison JA, et al. Metformin supplementation and life span in Fischer-344 rats. *J Gerontol A Biol Sci Med Sci.* 2010;65:468–474. doi:10.1093/gerona/gdq033
  22. Ravikumar B, Vacher C, Berger Z, et al. Inhibition of mTOR induces autophagy and reduces toxicity of polyglutamine expansions in fly and mouse models of Huntington disease. *Nat Genet.* 2004;36:585–595. PMID:15146184
  23. Kirkland JL. Perspectives on cellular senescence and short term dietary restriction in adults. *Aging (Albany NY).* 2010;2:894–896. PMID:21164220
  24. Das M, Gabriely I, Barzilai N. Caloric restriction, body fat and ageing in experimental models. *Obes Rev.* 2004;5(1):13–19. PMID:14969503
  25. Cunningham JT, Rodgers JT, Arlow DH, Vazquez F, Mootha VK, Puigserver P. mTOR controls mitochondrial oxidative function through a YY1-PGC-1 $\alpha$  transcriptional complex. *Nature.* 2007;450:736–740. doi:10.1038/nature06322
  26. Lamming DW, Ye L, Astle CM, Baur JA, Sabatini DM, Harrison DE. Young and old genetically heterogeneous HET3 mice on a rapamycin diet are glucose intolerant but insulin sensitive. *Aging Cell.* 2013;12:712–718. doi:10.1111/accel.12097
  27. Houde VP, Brûlé S, Festuccia WT, et al. Chronic rapamycin treatment causes glucose intolerance and hyperlipidemia by upregulating hepatic gluconeogenesis and impairing lipid deposition in adipose tissue. *Diabetes.* 2010;59:1338–1348. doi:10.2337/db09-1324
  28. Fang Y, Bartke A. Prolonged rapamycin treatment led to beneficial metabolic switch. *Aging (Albany NY).* 2013;5:328–329. PMID:3701104
  29. Miller RA, Harrison DE, Astle CM, et al. Rapamycin-mediated lifespan increase in mice is dose and sex dependent and metabolically distinct from dietary restriction. *Aging Cell.* December 17, 2013. [Epub ahead of print]. doi:10.1111/accel.12194
  30. Chen BJ, Morris RE, Chao NJ. Graft-versus-host disease prevention by rapamycin: cellular mechanisms. *Biol Blood Marrow Transplant.* 2000;6(5A):529–536. PMID:11071258
  31. Badman MK, Kennedy AR, Adams AC, Pissios P, Maratos-Flier E. A very low carbohydrate ketogenic diet improves glucose tolerance in ob/ob mice independently of weight loss. *Am J Physiol Endocrinol Metab.* 2009;297:E1197–E1204. doi:10.1152/ajpendo.00357.2009
  32. Wetter TJ, Gazdag AC, Dean DJ, Cartee GD. Effect of calorie restriction on in vivo glucose metabolism by individual tissues in rats. *Am J Physiol.* 1999;276(4 Pt 1):E728–E738. PMID:10198310
  33. Masoro EJ, McCarter RJ, Katz MS, McMahan CA. Dietary restriction alters characteristics of glucose fuel use. *J Gerontol.* 1992;47:B202–B208. PMID:1430849
  34. Huppe HC, Vanlerberghe GC, Turpin DH. Evidence for activation of the oxidative pentose phosphate pathway during photosynthetic assimilation of NO(3) but not NH(4) by a green alga. *Plant Physiol.* 1992;100:2096–2099. PMID:16653245
  35. Rezzi S, Martin FP, Shanmuganayagam D, Colman RJ, Nicholson JK, Weindruch R. Metabolic shifts due to long-term caloric restriction revealed in nonhuman primates. *Exp Gerontol.* 2009;44:356–362. doi:10.1016/j.exger.2009.02.008
  36. Boden G. Effects of free fatty acids (FFA) on glucose metabolism: significance for insulin resistance and type 2 diabetes. *Exp Clin Endocrinol Diabetes.* 2003;111:121–124. doi:10.1055/s-2003-39781
  37. Griffin ME, Marcucci MJ, Cline GW, et al. Free fatty acid-induced insulin resistance is associated with activation of protein kinase C  $\theta$  and alterations in the insulin signaling cascade. *Diabetes.* 1999;48:1270–1274. PMID:10342815
  38. Harber MP, Schenk S, Barkan AL, Horowitz JF. Alterations in carbohydrate metabolism in response to short-term dietary carbohydrate restriction. *Am J Physiol Endocrinol Metab.* 2005;289:E306–E312. doi:10.1152/ajpendo.00069.2005
  39. Johnston O, Rose CL, Webster AC, Gill JS. Sirolimus is associated with new-onset diabetes in kidney transplant recipients. *J Am Soc Nephrol.* 2008;19:1411–1418. doi:10.1681/ASN.2007111202
  40. Ma KL, Varghese Z, Ku Y, et al. Sirolimus inhibits endogenous cholesterol synthesis induced by inflammatory stress in human vascular smooth muscle cells. *Am J Physiol Heart Circ Physiol.* 2010;298:H1646–H1651. doi:10.1152/ajpheart.00492.2009
  41. Ma KL, Ruan XZ, Powis SH, Chen Y, Moorhead JF, Varghese Z. Sirolimus modifies cholesterol homeostasis in hepatic cells: a potential molecular mechanism for sirolimus-associated dyslipidemia. *Transplantation.* 2007;84:1029–1036. doi:10.1097/01.tp.0000286095.55685.e9
  42. Wieneke N, Hirsch-Ernst KI, Kuna M, Kersten S, Püschel GP. PPAR $\alpha$ -dependent induction of the energy homeostasis-regulating nuclear receptor NR1i3 (CAR) in rat hepatocytes: potential role in starvation adaptation. *FEBS Lett.* 2007;581:5617–5626. doi:10.1016/j.febslet.2007.11.011
  43. Shiraki T, Sakai N, Kanaya E, Jingami H. Activation of orphan nuclear constitutive androstane receptor requires subnuclear targeting by peroxisome proliferator-activated receptor gamma coactivator-1 alpha. A possible link between xenobiotic response and nutritional state. *J Biol Chem.* 2003;278:11344–11350. doi:10.1074/jbc.M212859200
  44. Corton JC, Brown-Borg HM. Peroxisome proliferator-activated receptor gamma coactivator 1 in caloric restriction and other models of longevity. *J Gerontol A Biol Sci Med Sci.* 2005;60:1494–1509. PMID:16424281
  45. Coburn CT, Knapp FF Jr, Febbraio M, Beets AL, Silverstein RL, Abumrad NA. Defective uptake and utilization of long chain fatty acids in muscle and adipose tissues of CD36 knockout mice. *J Biol Chem.* 2000;275:32523–32529. doi:10.1074/jbc.M003826200
  46. Pravenec M, Kazdová L, Landa V, et al. Transgenic and recombinant resistin impair skeletal muscle glucose metabolism in the spontaneously hypertensive rat. *J Biol Chem.* 2003;278:45209–45215. PMID:12944409